

# Negative- $U$ Anisotropic Charge Kondo Effect in a Triple Quantum Dot

Gwangsu Yoo,<sup>1</sup> Jinhong Park,<sup>1</sup> S.-S. B. Lee,<sup>1</sup> and H.-S. Sim<sup>1</sup>

<sup>1</sup>*Department of Physics, Korea Advanced Institute of Science and Technology, Daejeon 305-701, Korea*  
(Dated: June 22, 2021)

We predict a new type of the negative- $U$  Anderson impurity formed in a triple quantum dot. The two dots of the system behave as a negative- $U$  impurity preferring zero or double electron occupancy rather than single occupancy, and the third dot stabilizes the attractive interaction of  $U < 0$  via Coulomb repulsion. Using a bosonization method, we find that the system has the two different phases of massive or vanishing charge fluctuations between the two occupancies at low temperature, which are equivalent with the antiferromagnetic and ferromagnetic phases of the anisotropic Kondo model, respectively. The phase transition is experimentally accessible and identifiable by electron conductance, offering the possibility of experimentally exploring the anisotropic Kondo model.

PACS numbers: 73.63.Kv, 72.15.Qm, 71.10.Hf, 73.23.-b

A negative- $U$  Anderson impurity is a site at which two electrons interact attractively with negative charging energy  $U < 0$ , and prefers zero or double electron occupancy, rather than single occupancy. It was introduced by P. W. Anderson, to understand amorphous materials [1]. It results in unconventional superconductivity in PbTe doped with Tl [2–5], the charge Kondo effect [6, 7] of electron-pair fluctuations, and electron-pair tunneling in Josephson junctions [8, 9] or in molecules [10–13]. As it occurs in complex many-body situations [2, 14] or with phonons [10–13], it is not easy to experimentally study its unusual properties [4, 5].

On the other hand, a quantum dot is useful for studying [15–17] Kondo effects [18, 19], including the fractional shot noise [20, 21], the phase shift [22, 23], and Kondo cloud [24, 25]. Exotic Kondo effects [26, 27] and pseudospin resolved transport [28] were measured in a double dot. Triple quantum dots (TQDs) and larger systems are useful for artificially realizing magnetic effects [29–33] including a geometrical frustration effect [30].

The phase transition in the anisotropic Kondo effect, however, has not been experimentally explored in a controlled fashion. The transition occurs between the antiferromagnetic Kondo and ferromagnetic coupling phases. A single dot usually stays only in the Kondo phase. There have been the predictions of anisotropic Kondo effects in multiple dots [12, 31–36], but, they cover only a particular region of the phase diagram (e.g., only along the transition line [31–33]), or do not discuss experimental possibility. It will be valuable to find a setup for observing the phase transition and the ferromagnetic phase.

In this work, we predict a new type of the negative- $U$  impurity; see Fig. 1. It appears in a TQD, which has the two-fold degenerate ground states of charge configuration  $(n_A, n_B, n_C) = (1, 1, 0)$  and  $(0, 0, 1)$ ;  $n_i$  is electron occupation number in dot  $\lambda = A, B, C$ . Dot A and B of the TQD behave as a negative- $U$  site of  $n_A + n_B = 0$  or 2, and dot C stabilizes the attractive interaction of  $U < 0$  via Coulomb repulsion. Using bosonization and refermionization [37, 38], we find that the TQD has the two differ-

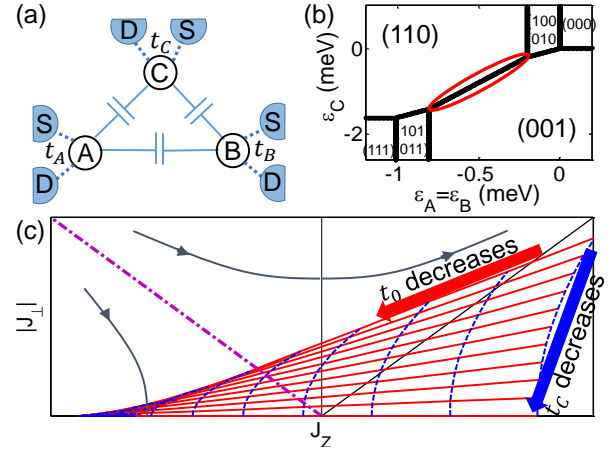


FIG. 1. (Color Online) (a) Schematic view of TQD. It has no inter-dot electron tunneling, while each dot ( $\lambda = A, B, C$ ) has tunneling strength  $t_\lambda$  to its own source S and drain D. (b) TQD Stability diagram. The degeneracy line of  $(1, 1, 0)$  and  $(0, 0, 1)$  is marked. We choose intra-dot Coulomb repulsion 8 meV, inter-dot repulsion  $U_{AB} = 0.2$  meV, and  $U_{0C} \equiv U_{AC} = U_{BC} = 0.8$  meV. (c) Kondo phase diagram with renormalization group flow (thin arrows) and phase transition (dash-dotted magenta). The shaded region is the anisotropy domain achievable with tuning  $t_0 \equiv t_A = t_B$  (along thick solid red arrow; one can tune only one of  $t_A$  and  $t_B$ ) and  $t_C$  (dashed blue), starting from a location of  $(J_z, J_\perp)$ .

ent phases of massive or vanishing fluctuations between the two ground states, which are equivalent with the two phases of the *anisotropic* Kondo effects. Our Kondo effect is unusual, as the change (pseudospin flip) from one to the other ground state is accompanied by *three* electron-tunneling events, each involving different dots. This causes the anisotropy, which is experimentally controllable with changing the tunneling strengths. Using numerical renormalization group (NRG) methods [39], we find that the two phases and the phase transition are experimentally accessible, and identifiable by electron conductance in a pseudospin-resolved fashion [28]. This offers the possibility of experimentally exploring the

anisotropic Kondo phase diagram that has not been experimentally confirmed yet. Note that the two-fold degeneracy was already observed [29, 30], and that the usual negative- $U$  impurities [6, 7] show only the antiferromagnetic isotropic Kondo phase, contrary to our case.

*Model.*— The three dots of the TQD repulsively interact but have no inter-dot electron tunneling; see Fig. 1. Its Hamiltonian is  $\mathcal{H} = \mathcal{H}_D + \mathcal{H}_T + \mathcal{H}_L$ . The dot part is  $\mathcal{H}_D = \sum_{\lambda=A,B,C} \epsilon_{\lambda} n_{\lambda} + \sum_{\lambda \neq \lambda'} U_{\lambda\lambda'} n_{\lambda} n_{\lambda'}$ . Electron number operator  $n_{\lambda} \equiv d_{\lambda}^{\dagger} d_{\lambda}$  is for the energy level  $\epsilon_{\lambda}$  of dot  $\lambda$  and  $U_{\lambda\lambda'} > 0$  is inter-dot Coulomb energy; we consider one orbital per dot. Each dot  $\lambda$  couples with its own two leads  $\lambda S$  and  $\lambda D$  via electron tunneling of strength  $t_{\lambda}$ , described by  $\mathcal{H}_T = \sum_{\lambda,k} t_{\lambda} c_{\lambda k}^{\dagger} d_{\lambda} + \text{H.c.}$   $c_{\lambda k}^{\dagger}$  creates an electron of momentum  $k$  and energy  $\epsilon_k$  in  $\lambda S$  and  $\lambda D$ ; we consider the symmetric case of  $c_{\lambda k}^{\dagger} = (c_{\lambda S k}^{\dagger} + c_{\lambda D k}^{\dagger})/\sqrt{2}$ ,  $c_{\lambda S(D)k}^{\dagger}$  being an operator for  $\lambda S(D)$ . The lead Hamiltonian is  $\mathcal{H}_L = \sum_{\lambda,k} \epsilon_k c_{\lambda k}^{\dagger} c_{\lambda k}$ ; we omit the lead states decoupled from the TQD. For simplicity, we choose the intradot Coulomb interaction  $\gg U_{\lambda\lambda'}$  (so double occupancy in dot level  $\epsilon_{\lambda}$  is ignored), and the symmetric case of  $\epsilon_A = \epsilon_B$ ,  $U_{0C} \equiv U_{AC} = U_{BC}$ , and  $t_0 \equiv t_A = t_B$ ; relaxing this simplification does not alter our results qualitatively. We ignore the spin of electrons and the ordinary spin Kondo effect in each dot, considering Zeeman energy (by a magnetic field) larger than the Kondo temperature of the spin Kondo effect;  $\epsilon_{\lambda}$  absorbs the Zeeman energy.

We impose the conditions for the two-fold degenerate ground states  $(0, 0, 1)$  and  $(1, 1, 0)$ . One is  $U_{AB} < U_{0C}$ , making the energy of  $(1, 1, 0)$  lower than that of the other double-occupancy states such as  $(1, 0, 1)$ . The others are  $-U_{0C} < \epsilon_{A/B} < -U_{AB}$ ,  $-2U_{0C} < \epsilon_C < 0$ , and  $\epsilon_A + \epsilon_B - \epsilon_C = -U_{AB}$ , achievable by gate voltages. For computational convenience, we consider the additional restrictions of  $\epsilon_A = \epsilon_B = -(U_{AB} + U_{0C})/2$  and  $\epsilon_C = -U_{0C}$ , making the spectral function particle-hole symmetric. We plot the stability diagram in Fig. 1.

The degenerate ground states prefer double or zero occupancy in dots A and B, as  $(n_A, n_B) = (1, 1)$  or  $(0, 0)$ , rather than single occupancy. So, A and B together behave as a negative- $U$  site, and C stabilizes it. A natural question is whether this negative- $U$  site shows a charge Kondo effect [6], massive charge fluctuations between its pseudospin states  $|\uparrow\rangle \equiv |n_A = 1, n_B = 1, n_C = 0\rangle$  and  $|\downarrow\rangle \equiv |0, 0, 1\rangle$ . We choose the pseudospin operators as  $S_z = [n_A n_B (1 - n_C) - (1 - n_A)(1 - n_B) n_C]/2$  and  $S_+ = d_A^{\dagger} d_B^{\dagger} d_C$ . Then,  $\mathcal{H}$  is mapped onto

$$\begin{aligned} \mathcal{H}_D + \mathcal{H}_T &\Rightarrow \mathcal{H}_0 \quad (1) \\ &= \sum_{kk'\lambda} J_{z\lambda} S_z c_{\lambda k}^{\dagger} c_{\lambda k'} + \sum_{kk'k''} (J_+ S_+ c_{Ck''}^{\dagger} c_{Bk'} c_{Ak} + \text{H.c.}), \\ J_{zA} = J_{zB} &= \frac{4t_0^2}{U_{0C} - U_{AB}} > 0, \quad J_{zC} = -\frac{2t_C^2}{U_{0C}} < 0, \\ J_+ &= -8t_0^2 t_C \left( \frac{1}{U_{0C}(U_{0C} - U_{AB})} + \frac{1}{(U_{0C} - U_{AB})^2} \right) \end{aligned}$$

by the Schrieffer-Wolff transformation [19].  $\mathcal{H}_0$  has three species ( $\lambda = A, B, C$ ) of electrons, contrary to the usual Kondo model of two species (spin up, down).

*Bosonization and refermionization.*— It is nontrivial whether  $\mathcal{H}_0$  shows a Kondo effect. To see this, we apply a bosonization method [37, 38, 46], where the field operator  $c_{\lambda}^{\dagger}(0) = \sqrt{2\pi/L} \sum_k c_{\lambda k}^{\dagger}$  at  $x = 0$  (the position coupled to dot  $\lambda$ ) in lead  $\lambda$  is bosonized as  $c_{\lambda}^{\dagger}(0) = e^{i\theta_{\lambda}} e^{i\phi_{\lambda}(0)}/\sqrt{a}$ . Here,  $e^{i\theta_{\lambda}}$  is the Klein factor of lead  $\lambda$ ,  $\phi_{\lambda}(x)$  are the bosonic field describing plasmon excitations in lead  $\lambda$ ,  $a$  is the short-distance cutoff, and each lead is treated as a one-dimensional wire of length  $L$ .  $\mathcal{H}_0$  is bosonized,

$$\begin{aligned} \mathcal{H}_0 &= \frac{L}{2\pi} \sum_{\lambda=A,B,C} J_{z\lambda} S_z (\partial_x \phi_{\lambda}(0) + \frac{2\pi N_{\lambda}}{L}) + \left(\frac{L}{2\pi a}\right)^{3/2} \\ &\times J_+ S_+ e^{i\theta_C} e^{-i\theta_B} e^{-i\theta_A} e^{i(\phi_C(0) - \phi_B(0) - \phi_A(0))} + \text{H.c.} \end{aligned}$$

In the first term,  $\partial_x \phi_{\lambda}(0) + 2\pi N_{\lambda}/L$  means electron density at  $x = 0$  in lead  $\lambda$ , where  $N_{\lambda}$  is the total number of electrons in lead  $\lambda$ ; we omit the normal ordering.

In the pseudospin flip  $|\uparrow\rangle \leftrightarrow |\downarrow\rangle$ ,  $N_C + (N_A + N_B)/2$  and  $N_A - N_B$  are conserved, as  $(N_A, N_B, N_C)$  change by  $(-1, -1, 1)$  or  $(1, 1, -1)$ . Using this, we introduce pseudofermion numbers  $N_{\uparrow}, N_{\downarrow}, N_x$ .  $N_{\uparrow(\downarrow)}$  counts the pseudospin-up (down) fermions that try to screen impurity pseudospin  $\downarrow$  ( $\uparrow$ ), while  $N_x = r_1[N_C + (N_A + N_B)/2]$  counts the fermions irrelevant to the screening. We choose  $N_{\uparrow} + N_{\downarrow} = r_2(N_A - N_B)$ , as the corresponding number is conserved in the spin-1/2 Kondo effect. Here,  $r_{1,2}$  are constants. We choose  $N_{\uparrow} - N_{\downarrow} = (2/3)(N_A + N_B - N_C)$  from the analogy that  $N_A + N_B - N_C$  changes by 3 in the pseudospin flip, while the corresponding number change is 2 in the spin-1/2 Kondo effect. Hence,

$$\begin{aligned} (N_{\uparrow}, N_{\downarrow}, N_x)^{\top} &= M(N_A, N_B, N_C)^{\top}, \quad (2) \\ M &= \frac{2}{3} \begin{pmatrix} (1-l)/2 & (1+l)/2 & -\frac{1}{2} \\ -(1+l)/2 & -(1-l)/2 & \frac{1}{2} \\ \frac{1}{2} & \frac{1}{2} & 1 \end{pmatrix} \text{ and } l = \sqrt{\frac{3}{2}}, \end{aligned}$$

where  $\top$  means matrix transpose. We have chosen  $r_{1,2}$  such that  $M$  is proportional to a unitary matrix (which is  $lM$ ). We define the Klein factors,  $\exp(i\theta_{\uparrow,\downarrow,x})$ , and boson fields of the pseudofermions corresponding to  $N_{\uparrow,\downarrow,x}$ ,

$$\begin{aligned} (\theta_{\uparrow}, \theta_{\downarrow}, \theta_x)^{\top} &= l^2 M(\theta_A, \theta_B, \theta_C)^{\top}, \\ (\phi_{\uparrow}, \phi_{\downarrow}, \phi_x)^{\top} &= lM(\phi_A, \phi_B, \phi_C)^{\top}. \quad (3) \end{aligned}$$

The Klein factors are determined by commutators  $[\theta_{\lambda}, N_{\lambda'}] = i\delta_{\lambda\lambda'}$ ,  $\lambda \in \{A, B, C\}$  or  $\{\uparrow, \downarrow, x\}$ , while the unitary matrix  $lM$  is chosen for the bosons  $\phi_{\uparrow,\downarrow,x}$ , since the boson transformation should be unitary; the choice is justified by the following successful refermionization.

Using Eq. (2), we write  $\mathcal{H}_0$  as

$$\begin{aligned} \mathcal{H}_0 &= \frac{L}{2\pi} \frac{1}{l} (J_{zA} - \frac{J_{zC}}{2}) S_z \sum_{\sigma=\uparrow,\downarrow} w_{\sigma} (\partial_x \phi_{\sigma}(0) + l \frac{2\pi N_{\sigma}}{L}) \\ &+ \left(\frac{L}{2\pi a}\right)^{3/2} e^{i\pi \frac{l-1}{2}} J_+ S_+ e^{i\theta_{\downarrow}} e^{-i\theta_{\uparrow}} e^{il[\phi_{\downarrow}(0) - \phi_{\uparrow}(0)]} + \text{H.c.}, \end{aligned}$$

where  $w_\uparrow = 1$ ,  $w_\downarrow = -1$ , and we used  $J_{zA} = J_{zB}$ . Here, we omit the term of  $\frac{L}{2\pi} \frac{1}{l} S_z (J_{zA} + J_{zC}) (\partial_x \phi_x(0) + l 2\pi N_x / L)$ , which is marginal in Poorman's scaling (so it does not influence the Kondo effect of  $\mathcal{H}_0$ ), since the pseudospin flip does not modify  $N_x$  and  $\phi_x$ .

We apply the Emery-Kivelson transformation [37, 38] of  $U_{EK} = e^{i\pi[-(l/2)N_\uparrow + ((2-l)/2)N_\downarrow]S_z} e^{i(l-1)S_z(\phi_\uparrow(0) - \phi_\downarrow(0))}$  to refermionize  $\mathcal{H}_0 + \mathcal{H}_L$  by  $\mathcal{H}_K = U_{EK}(\mathcal{H}_0 + \mathcal{H}_L)U_{EK}^\dagger$ . This leads to the *anisotropic* Kondo Hamiltonian [46],

$$\mathcal{H}_K = 2J_z S_z s_z + J_\perp (S_+ s_- + \text{H.c.}) + \sum_{k\sigma} \tilde{\epsilon}_{k\sigma} f_{k\sigma}^\dagger f_{k\sigma},$$

$$J_z \equiv \frac{1}{l} (J_{zA} - \frac{J_{zC}}{2}) - \frac{l-1}{\rho}, \quad J_\perp \equiv \sqrt{\frac{L}{2\pi a}} J_+. \quad (4)$$

$f_{k\sigma}^\dagger$  creates a refermionized fermion with spin  $\sigma$ , momentum  $k$ , and energy  $\tilde{\epsilon}_k$ ,  $s_z$  and  $s_\pm = s_x \pm i s_y$  are the spin operators of the fermions ( $f_{k\sigma}^\dagger$ ) coupled to the TQD pseudospin, and  $\rho$  is the density of states of leads  $\lambda$ . The term  $-(l-1)/\rho$  is contributed from the fermion spin effectively bound to the TQD pseudospin.

In Eq. (4),  $J_z$  can be negative, with the help of  $-(l-1)/\rho < 0$ . By tuning  $J_z$  and  $J_\perp$  (namely,  $t_0$  and  $t_C$ ; see Eq. (1)), it is possible to reach both the antiferromagnetic Kondo and ferromagnetic phases, crossing the transition between them; see Figs. 2(a). In the antiferromagnetic phase, charge fluctuations (pseudo-spin flip) between the two ground states massively occur at low temperature, while they vanish in the ferromagnetic phase.

*Phase transition.*— To confirm the charge Kondo effect and the phase transition, we apply NRG methods [39] to the initial Hamiltonian  $\mathcal{H}$  (Anderson model), with the parameters close to recent experiments [28]; we choose the bandwidth  $D$  of the leads as  $D = 1$  eV. We compute differential electron conductance  $G_\lambda$  through dot  $\lambda$ , applying bias  $V \rightarrow 0$  to lead  $\lambda S$ ; the other leads of  $\lambda D$ ,  $\lambda' S$ , and  $\lambda' D$  ( $\lambda' \neq \lambda$ ) are unbiased. Figure 2 shows  $G_A$  and  $G_C$ . At  $t_0 = t_C = 11$  meV [the corresponding  $(J_z, J_\perp)$  is marked by cross in Fig. 2(a)], the spectral function (not shown here) and  $G_\lambda$  (see Ref. [46]) show that the TQD is in the Kondo phase and has Kondo temperature  $T_K \gtrsim 150$  mK, which is achievable in current experiments. Here,  $T_K = D[(J_z + \Delta_J)/(J_z - \Delta_J)]^{-1/(4\rho\Delta_J)}$  and  $\Delta_J = \sqrt{J_z^2 - J_\perp^2}$ ;  $T_K \rightarrow D e^{-1/(2\rho J_z)}$  in the  $J_z = J_\perp$  limit.

As  $t_0$  decreases, with  $t_C = 11$  meV fixed, the TQD moves to the ferromagnetic phase, crossing the phase transition. The transition is identified by the dependence of  $G_\lambda$  on temperature  $T$ ; see Fig. 2. In the Kondo regime,  $G_\lambda$  increases as  $T$  decreases;  $G_\lambda \propto 1 - (\pi T/T_K)^2$  at  $T \ll T_K$ . In contrast, not in the Kondo phase, namely in both the antiferromagnetic region of  $T > T_K$  (the red square and diamond in Fig. 2) and the ferromagnetic phase (star and circle), we find the  $T$  dependence [46],

$$G_\lambda \propto \left( \Delta_J \frac{1 + (T/T_K)^{-4\rho\Delta_J}}{1 - (T/T_K)^{-4\rho\Delta_J}} + m_\lambda \right)^2 + n_\lambda \quad (5)$$

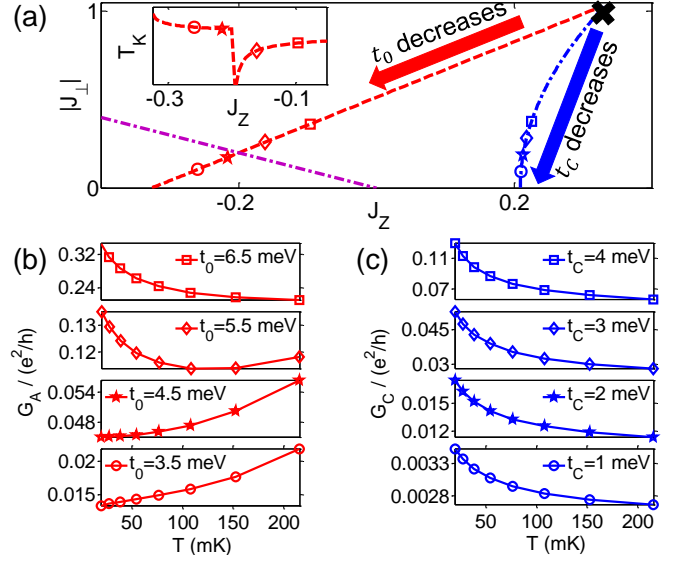


FIG. 2. (Color online) NRG results of differential conductance  $G_{A(C)}$  through dot A (C). (a)  $(J_z, J_\perp)$ 's, at which  $G_{A(C)}$  is computed in (b) and (c), are marked by symbols. They are selected, starting from  $t_0 = t_C = 11$  meV (marked by cross) and lowering  $t_0$  (along red dashed trajectory) or  $t_C$  (blue dashed-dot). The other parameters such as  $U_{\lambda\lambda'}$  are the same with those in Fig. 1. In this choice, the trajectory crosses the phase transition (solid line) as  $t_0$  decreases, while it stays within the Kondo phase as  $t_C$  varies. Inset:  $T_K$  along the trajectory of lowering  $t_0$ . It shows a jump at the transition. (b) The dependence of  $G_A$  on  $T$  at different  $t_0$ 's, with fixed  $t_C = 11$  meV along the red dashed trajectory of (a). (c)  $G_C(T)$  at different  $t_C$ 's, with fixed  $t_0 = 11$  meV along the blue dash-dot trajectory of (a). In the ferromagnetic (antiferromagnetic Kondo) phase,  $G_{A,C}$  becomes smaller (larger) as  $T$  decreases.

where  $m_\lambda$  and  $n_\lambda$  are  $T$ -independent; their expressions are found in Ref. [46], and  $G_\lambda = (1/\ln(T/T_K) + m_\lambda)^2 + n_\lambda$  when  $J_z = J_\perp$  [15]. In the ferromagnetic phase,  $G_\lambda$  increases as  $T$  increases, showing the opposite behavior to the Kondo phase. Note that the ferromagnetic phase is also characterized by  $T_K$ , although  $T_K$  has a different meaning from the Kondo phase, and has the spectral function  $\propto [\ln(\omega/T_K)]^{-2}$  increasing with energy  $\omega$  [40]; the jump of  $T_K$  at the transition is shown in the inset of Fig. 2(a). Around the transition,  $G_\lambda$  shows the crossing behavior between the two opposite  $T$  dependence.

On the other hand, as  $t_C$  decreases, with  $t_0 = 11$  meV fixed, the TQD stays in the Kondo phase, so that  $G_\lambda$  increases as  $T$  decreases. The  $T$  dependence of  $G_\lambda$  and  $T_K$  at different  $t_0$ 's and  $t_C$ 's will be useful for experimentally studying the charge Kondo effect and the Kondo phase transition in the TQD. Note that as we choose the parameters of  $\mathcal{H}$  close to experiments [28],  $G_\lambda$  is affected by the tails of Coulomb blockade resonances of  $\mathcal{H}$  in Fig. 2; in Fig. 2(b),  $G_A$  shows nonzero value at  $T \rightarrow 0$  in the ferromagnetic phase due to the tails, and we plot  $G_A$ , instead of  $G_C$ , as the former is less affected by the tails.

*Isotropic regime.*— In the Kondo phase, the TQD approaches, at low enough  $T$ , to the strong coupling fixed point of the isotropic Kondo effect. Applying Eq. (3) to the standard fixed-point Hamiltonian [41, 46], we derive the effective fixed-point Hamiltonian of the charge Kondo effect of three electron species  $\lambda = A, B, C$  as

$$\mathcal{H}_{\text{fp}} = \mathcal{H}_L - \frac{1}{2\pi\rho T_K} \sum_{\lambda=A,B,C;k,k'} \alpha_\lambda (\epsilon_k + \epsilon_{k'}) c_{\lambda k}^\dagger c_{\lambda k'} + \frac{1}{\pi\rho^2 T_K} \sum_{\lambda' \neq \lambda; k_1 k_2 k_3 k_4} \beta_{\lambda\lambda'} c_{\lambda k_1}^\dagger c_{\lambda k_2} c_{\lambda' k_3}^\dagger c_{\lambda' k_4}, \quad (6)$$

where  $\alpha_A = \alpha_B = \alpha_C = 2/3$ ,  $\beta_{AB} = -2/3$ , and  $\beta_{AC} = \beta_{BC} = 2/3$ . The  $\alpha_\lambda$  terms describe elastic scattering, while  $\beta_{\lambda\lambda'}$  the inelastic scattering destroying the Kondo singlet. Interestingly, the sign of  $\beta_{\lambda\lambda'}$  carries the information whether the inter-dot interaction is repulsive or attractive.  $\beta_{AC(BC)} > 0$  means the repulsive interaction between dot A (B) and C, while  $\beta_{AB} < 0$  comes from the negative- $U$  interaction between A and B.

Observables depend on  $\alpha_\lambda$  and  $\beta_{\lambda\lambda'}$  in the Kondo phase, in a different way from usual Kondo effects. Below, we apply bias voltages  $V_\lambda$  to leads  $\lambda S$ , satisfying  $k_B T \ll V_A, V_B, V_C \ll k_B T_K$ . From Eq. (6) and following Refs. [41, 42], we obtain the phase shift of electrons of energy  $\epsilon$  and species  $\lambda$ , scattered by the Kondo resonance,

$$\delta_\lambda = \frac{\pi}{2} + \alpha_\lambda \frac{\epsilon}{T_K} - \sum_{\lambda' \neq \lambda} \beta_{\lambda\lambda'} \frac{eV_{\lambda'}}{T_K}. \quad (7)$$

From  $d\delta_\lambda/dV_{\lambda'}$ , one can experimentally [22, 23] measure  $\beta_{\lambda\lambda'}$  and confirm the negative- $U$  site by  $\beta_{AB} < 0$ .

We also derive, using Keldysh formalism [20], electron current through dot  $\lambda$  as [up to  $O(V^3)$ ]

$$I_\lambda = \frac{e^2}{h} [V_\lambda - (\frac{\alpha_\lambda^2}{12} + \sum_{\lambda' \neq \lambda} \frac{\beta_{\lambda\lambda'}^2}{6}) \frac{e^2 V_\lambda^3}{T_K^2} - \sum_{\lambda' \neq \lambda} \frac{\beta_{\lambda\lambda'}}{4} \frac{e^2 V_\lambda V_{\lambda'}}{T_K^2}]. \quad (8)$$

For  $V_\lambda = 0$ ,  $I_\lambda$  vanishes even if  $V_{\lambda' \neq \lambda} \neq 0$ . Using conductance  $G_\lambda = dI_\lambda/dV_\lambda$  and transconductance  $G_{\lambda\lambda'} = dI_\lambda/dV_{\lambda'}$ , one can experimentally obtain  $\alpha^2$  and  $\beta^2$ , the information of the scattering in the Kondo effects. Hence, our TQD is useful for studying the Kondo effect, by measuring the single-particle observable of  $I_\lambda$  in a pseudo-spin resolved fashion [28]. Note that similar information can be obtained from shot noise [20, 21], a two-particle observable.

*Summary.*— We have shown that a new type of the negative- $U$  impurity appears in a TQD. It results in an anisotropic charge Kondo effect with tunable anisotropy. Interestingly, this pseudospin-1/2 Kondo effect is accompanied by three different electron species (dot A, B, C) contrary to the usual Kondo effect of two species (spin up, down). The TQD is useful for studying the Kondo phase transition, the ferromagnetic phase, a negative- $U$  feature, and the inelastic Kondo scattering in a pseudospin-resolved fashion [28]. Note that our charge Kondo effect

has a different origin from those by orbitals [28, 43, 44], and that the TQD is the minimal quantum dot system possessing a negative- $U$  site. Larger systems such as a quadruple dot can also host a negative- $U$  site [45].

We thank Yunchul Chung, David Goldhaber-Gordon, and especially Yuval Oreg for discussion. This work was supported by Korea NRF (Grant No. 2011-0022955, Grant No. 2013R1A2A2A01007327).

- 
- [1] P. W. Anderson, Phys. Rev. Lett. **34**, 953 (1975).
  - [2] C. M. Varma, Phys. Rev. Lett. **61**, 2713 (1988).
  - [3] M. Dzero and J. Schmalian, Phys. Rev. Lett. **94**, 157003 (2005).
  - [4] T. A. Costi and V. Zlatic, Phys. Rev. Lett. **108**, 036402 (2012).
  - [5] Y. Matsushita, H. Bluhm, T. H. Geballe, and I. R. Fisher, Phys. Rev. Lett. **94**, 157002 (2005).
  - [6] A. Taraphder and P. Coleman, Phys. Rev. Lett. **66**, 2814 (1991).
  - [7] J. Koch, E. Sela, Y. Oreg, and F. von Oppen, Phys. Rev. B **75**, 195402 (2007).
  - [8] V. Oganesyan, S. Kivelson, T. Geballe, and B. Mozyzhes, Phys. Rev. B **65**, 172504 (2002).
  - [9] V. I. Kozub, A. V. Lopatin, and V. M. Vinokur, Phys. Rev. Lett. **90**, 226805 (2003).
  - [10] J. Koch, M. E. Raikh, and F. von Oppen, Phys. Rev. Lett. **96**, 056803 (2006).
  - [11] A. S. Alexandrov, A. M. Bratkovsky, and R. S. Williams, Phys. Rev. B **67**, 075301 (2003).
  - [12] P. S. Cornaglia, H. Ness, and D. R. Grempel, Phys. Rev. Lett. **93**, 147201 (2004).
  - [13] S. Andergassen, T. A. Costi, and V. Zlatic, Phys. Rev. B **84**, 241107(R) (2011).
  - [14] I. E. Perakis and C. M. Varma, Phys. Rev. B **49**, 9041 (1994).
  - [15] M. Pustilnik and L. Glazman, J. Phys.: Condens. Matter **16**, R513 (2004).
  - [16] D. Goldhaber-Gordon, H. Shtrikman, D. Mahalu, D. Abusch-Magder, U. Meirav, and M. A. Kastner, Nature **391** 156 (1998).
  - [17] S. M. Cronenwett, T.H. Oosterkamp, and L.P. Kouwenhoven, Science **281**, 540 (1998).
  - [18] J. Kondo, Prog. Theor. Phys., **32**, 37 (1964).
  - [19] A. C. Hewson, *The Kondo problem to heavy fermions*, Cambridge Studies in Magnetism (Cambridge University Press, Cambridge, 1993).
  - [20] E. Sela, Y. Oreg, F. von Oppen, and J. Koch, Phys. Rev. Lett. **97**, 086601 (2006).
  - [21] Y. Yamauchi *et al.*, Phys. Rev. Lett. **106**, 176601 (2011).
  - [22] Y. Ji, M. Heiblum, D. Sprinzak, D. Mahalu, and H. Shtrikman, Science **290**, 779 (2000).
  - [23] S. Takada *et al.*, cond-mat/1311.6884 (2013).
  - [24] I. Affleck, in *Perspectives of Mesoscopic Physics* (World Scientific, 2010), pp. 1-44.
  - [25] J. Park, S.-S. B. Lee, Y. Oreg, and H.-S. Sim, Phys. Rev. Lett. **110**, 246603 (2013).
  - [26] H. Jeong, A. M. Chang, and M. R. Melloch, Science **293**, 2221 (2001).
  - [27] R. M. Potok, I. G. Rau, H. Shtrikman, Y. Oreg, and D.

- Goldhaber-Gordon, *Nature* **446**, 167 (2007).
- [28] S. Amasha *et al.*, *Phys. Rev. Lett.* **110**, 046604 (2013).
  - [29] M. C. Rogge and R. J. Haug, *Phys. Rev. B* **77**, 193306 (2008).
  - [30] M. Seo *et al.*, *Phys. Rev. Lett.* **110**, 046803 (2013).
  - [31] T. Kuzmenko, K. Kikoin, and Y. Avishai, *Phys. Rev. B* **73**, 235310 (2006).
  - [32] A. K. Mitchell, T. F. Jarrold, and D. E. Logan, *Phys. Rev. B* **79**, 085124 (2009).
  - [33] P. P. Baruselli, R. Requist, M. Fabrizio, and E. Tosatti, *Phys. Rev. Lett.* **111**, 047201 (2013).
  - [34] M. Garst, S. Kehrein, T. Pruschke, A. Rosch, and M. Vojta, *Phys. Rev. B* **69**, 214413 (2004).
  - [35] C. Romeike, M. R. Wegewijs, W. Hofstetter, and H. Schoeller, *Phys. Rev. Lett.* **96**, 196601 (2006).
  - [36] M. Pletyukhov, D. Schuricht, and H. Schoeller, *Phys. Rev. Lett.* **104**, 106801 (2010).
  - [37] V. J. Emery and S. A. Kivelson, *Phys. Rev. Lett.* **71**, 3701 (1993).
  - [38] J. von Delft and H. Schoeller, *Annalen Phys.* **7**, 225 (1998).
  - [39] R. Bulla, T. A. Costi, and T. Pruschke, *Rev. Mod. Phys.* **80**, 395 (2008).
  - [40] W. Koller, A. C. Hewson, and D. Meyer, *Phys. Rev. B* **72**, 045117 (2005).
  - [41] P. Nozières, *J. Low Temp. Phys.* **17**, 31 (1974); *J. Phys. (Paris)* **39**, 1117 (1978).
  - [42] C. Mora, P. Vitushinsky, X. Leyronas, A. A. Clerk, and K. Le Hur, *Phys. Rev. B* **80**, 155322 (2009).
  - [43] L. Borda, G. Zaránd, W. Hofstetter, B.I. Halperin, and J. von Delft, *Phys. Rev. Lett.* **90**, 026602 (2003).
  - [44] M. R. Galpin, D. E. Logan, and H. R. Krishnamurthy, *Phys. Rev. Lett.* **94**, 186406 (2005).
  - [45] Private communication with Yuval Oreg.
  - [46] See Supplementary Material for the details.

# Supplementary Material for “Negative- $U$ Anisotropic Charge Kondo Effect in a Triple Quantum Dot”

Gwangsu Yoo,<sup>1</sup> Jinhong Park,<sup>1</sup> S.-S. B. Lee,<sup>1</sup> and H.-S. Sim<sup>1</sup>

<sup>1</sup>*Department of Physics, Korea Advanced Institute of Science and Technology, Daejeon 305-701, Korea*  
(Dated: June 22, 2021)

In this Supplementary Material, we provide the expression of  $\mathcal{H}_L$  in the bosonization, the details of the refermionization in Eq. (4), the dependence of  $G_{A(C)}$  on  $t_{0(C)}$ , and the derivation of Eqs. (5) and (6) of the main text.

We first provide the expression of  $\mathcal{H}_L = \sum_{\lambda k} \epsilon_k c_{\lambda k}^\dagger c_{\lambda k}$  in the bosonization, which is skipped in the main text. After the unitary transformation of Eq. (3), we have

$$\mathcal{H}_L = \hbar v_F \sum_{\lambda=A,B,C} \int_{-L/2}^{L/2} \frac{dx}{2\pi} \frac{1}{2} (\partial_x \phi_\lambda(x))^2 = \hbar v_F \sum_{\sigma=\uparrow,\downarrow,X} \int_{-L/2}^{L/2} \frac{dx}{2\pi} \frac{1}{2} (\partial_x \phi_\sigma(x))^2.$$

Next, we discuss the refermionization details in the derivation of Eq. (4). We apply the Emery-Kivelson transformation  $U_{EK}$  to the total Hamiltonian of  $\mathcal{H}_L + \mathcal{H}_0$  as  $U_{EK}(\mathcal{H}_L + \mathcal{H}_0)U_{EK}^\dagger$ . This results in

$$U_{EK}(\mathcal{H}_L + \mathcal{H}_{0,z})U_{EK}^\dagger = \mathcal{H}_L + \mathcal{H}_{0,z} - \frac{(l-1)L}{2\pi\rho} S_z \sum_{\sigma=\uparrow,\downarrow} w_\sigma \partial_x \phi_\sigma(0),$$

$$U_{EK}\mathcal{H}_{0,\perp}U_{EK}^\dagger = \left(\frac{L}{2\pi a}\right)^{3/2} J_+ S_+ F_\downarrow^\dagger F_\uparrow e^{i[\phi_\downarrow(0) - \phi_\uparrow(0)]}$$

where  $\mathcal{H}_0 = \mathcal{H}_{0,z} + \mathcal{H}_{0,\perp}$ ,

$$\mathcal{H}_{0,z} = \frac{L}{2\pi} \frac{1}{l} \left( J_{zA} - \frac{J_{zC}}{2} \right) S_z \sum_{\sigma=\uparrow,\downarrow} w_\sigma (\partial_x \phi_\sigma(0) + l \frac{2\pi N_\sigma}{L})$$

$$\mathcal{H}_{0,\perp} = \left(\frac{L}{2\pi a}\right)^{3/2} e^{i\pi \frac{l-1}{2}} J_+ S_+ e^{i\theta_\downarrow} e^{-i\theta_\uparrow} e^{il[\phi_\downarrow(0) - \phi_\uparrow(0)]} + \text{H.c.}.$$

The Klein factors in the EK transformed Hamiltonian are defined as

$$F_\downarrow^\dagger \equiv e^{i(\theta_\downarrow - \frac{l-1}{2}\pi N_\uparrow)},$$

$$F_\uparrow^\dagger \equiv e^{i(\theta_\uparrow + \frac{l-1}{2}\pi N_\downarrow)}.$$

and a phase shifted operator for a dot  $\lambda$  can be written as

$$d_\lambda \rightarrow e^{-i\frac{\pi}{2}S_z} d_\lambda e^{i\frac{\pi}{2}(S_z + N_\uparrow - N_\downarrow)},$$

which are satisfying  $\{d_\lambda, F_\sigma\} = 0$  and  $[N_\sigma, F_\sigma] = -F_\sigma$ . Here,  $n_\lambda$  is the occupation number of the dot level  $\epsilon_\lambda$ ,  $N_\sigma$  is the total number of pseudofermion in lead  $\sigma$ , and we have used the relation of  $\rho = L/(2\pi\hbar v_F)$  in the computation of  $U_{EK}(\mathcal{H}_L + \mathcal{H}_{0,z})U_{EK}^\dagger$ . Then, we are ready to refermionize the transformed Hamiltonian of  $U_{EK}(\mathcal{H}_L + \mathcal{H}_0)U_{EK}^\dagger$ . We introduce the pseudofermion operator  $f_\sigma(x=0)$  corresponding to the pseudofermion number  $N_\sigma$  as

$$f_\sigma(0) \equiv \frac{F_\sigma}{\sqrt{a}} e^{-i\phi_\sigma(0)}, \quad f_\sigma^\dagger(0)f_\sigma(0) = \partial_x \phi_\sigma(0) + l\Delta_L N_\sigma. \quad (\text{S1})$$

Combining this with  $U_{EK}(\mathcal{H}_L + \mathcal{H}_0)U_{EK}^\dagger$  and  $F_{\uparrow,\downarrow}^\dagger$ , we obtain Eq. (4).

Next, in Fig. S1, we plot the the dependence of  $G_{A(C)}$  on  $t_{0(C)}$  at different temperatures. The differential conductance approaches to the unitary limit of  $e^2/h$  at low temperature in the Kondo phase; we ignore the spin degree of freedom, considering a finite Zeeman energy. And, around  $t_0 = t_C = 11$  meV, the Kondo temperature is obtained as about 150 mK, which is experimentally achievable. In Fig. S1(c),  $G_A$  shows the crossing behavior around the transition between the antiferromagnetic and ferromagnetic phases, which is supplementary to Fig. 2(b).

Next, we derive Eq. (5). Conductance  $G_\lambda$  is obtained, using t-matrix  $\mathcal{T}_\lambda$ , as [1]

$$G_\lambda = G_0 \int d\omega \left(-\frac{df}{d\omega}\right) \frac{1}{2} [-\pi\rho \text{Im}\mathcal{T}_\lambda(\omega)],$$

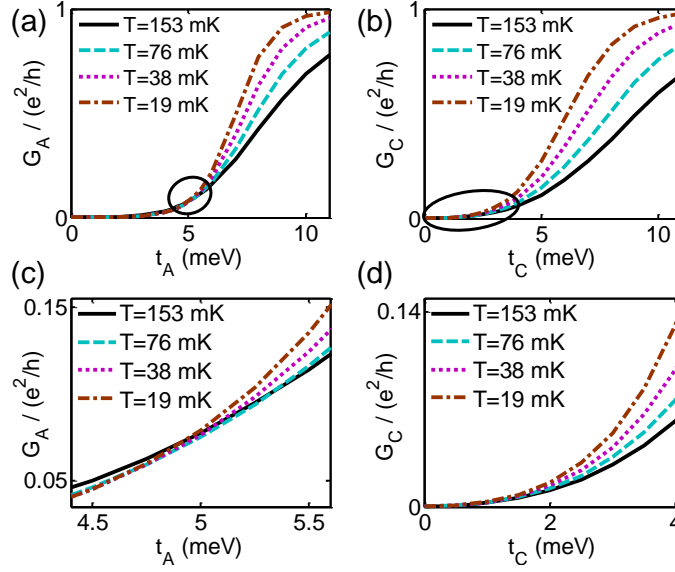


FIG. S1: (a) Dependence of  $G_A$  on  $t_0$  at different temperatures  $T$ , with fixed  $t_C = 11$  meV, along the red dashed trajectory of Fig. 2(a). (b) Dependence of  $G_C$  on  $t_C$  at different temperatures  $T$ , with fixed  $t_0 = 11$  meV, along the blue dash-dot trajectory of Fig. 2(a). The marked regions of (a) and (b) are magnified in (c) and (d), respectively.

where  $f$  is the Fermi-Dirac distribution function of energy  $\omega$  and  $\rho$  is the density of states in the leads. Applying the optical theorem and using the transition amplitude [1]  $\mathcal{A}_{|k'\lambda',\sigma'\rangle \leftarrow |k\lambda,\sigma\rangle}$  of reservoir states due to the scattering by the TQD, we write

$$\text{Im}\mathcal{T}_\lambda \propto \sum_{\sigma,\sigma',\lambda'} |\mathcal{A}_{|k'\lambda',\sigma'\rangle \leftarrow |k\lambda,\sigma\rangle}|^2.$$

After some straightforward calculations and by putting the coefficients of Eq. (1) and Eq. (4), we find

$$\text{Im}\mathcal{T}_\lambda \propto \frac{1}{2} J_{z\lambda}^2(\omega) + J_+^2(\omega) \propto (J_z(\omega) + m_\lambda)^2 + n_\lambda$$

where  $m_\lambda = \chi^2 \zeta_\lambda / (2l^2 + \chi^2)$ ,  $n_\lambda = (2l^2 \zeta_\lambda^2 \chi^2 - 4l^4 \Delta_J^2 - 2l^2 \Delta_J^2 \chi^2) / (2l^2 + \chi^2)^2$ ,  $\zeta_{A,B} = l(J_{zA,zB} + J_{zC})/3 + (l-1)/\rho$ ,  $\zeta_C = -(J_{zA} + J_{zC})/l + (l-1)/\rho$ , and  $\chi = \sqrt{L/(2\pi a)}$ . Note that  $m_\lambda$  and  $n_\lambda$  are independent on  $T$ , because  $J_{zA} + J_{zC}$  is a coefficient of the marginal term in Poorman's scaling. Using an expression,  $J_z(T) = \Delta_J(1 + (T/T_K)^{-4\rho\Delta_J})/(1 - (T/T_K)^{-4\rho\Delta_J})$  from Poorman's scaling, we obtain Eq. (5).

Finally, we discuss the derivation of Eq. (6). The strong-coupling fixed point Hamiltonian for the usual spin-1/2 Kondo model is written as [2]

$$\mathcal{H} = \mathcal{H}_L - \frac{1}{2\pi\rho T_K} \sum_{\sigma=\uparrow,\downarrow;k,k'} (\epsilon_k + \epsilon_{k'}) f_{\sigma k}^\dagger f_{\sigma k'} + \frac{1}{\pi\rho^2 T_K} \sum_{k_1,k_2,k_3,k_4} f_{\uparrow k_1}^\dagger f_{\uparrow k_2} f_{\downarrow k_3}^\dagger f_{\downarrow k_4}, \quad (\text{S2})$$

where  $f_{k\sigma}^\dagger$  creates an electron with momentum  $k$  and spin  $\sigma$  in a reservoir. In our case,  $f_{k\sigma}$  is the pseudofermion operator defined in Eq. (4). Using Eq. (S1), we rewrite the Hamiltonian in Eq. (S2) in terms of  $\phi_\sigma$  and  $N_\sigma$ . Then, using the transformation in Eqs. (2) and (3), the Hamiltonian is expressed in terms of the operators of lead  $\lambda$ , which leads to Eq. (6).

[1] M. Pustilnik and L. Glazman, J. Phys.: Condens. Matter **16**, R513 (2004).

[2] P. Nozières, J. Low Temp. Phys. **17**, 31 (1974); J. Phys. (Paris) **39**, 1117 (1978).